Indication of a mass-dependent anisotropy above $10^{18.7}$ eV in the hybrid data of the Pierre Auger Observatory

Cosmic Ray Indirect – Contribution 630

Discussion on July 13th @ 18 00 CEST

Eric Mayotte[a] on behalf of the Pierre Auger Collaboration[b]

spokespersons@auger.org

[a] Bergische Universität Wuppertal, Department of Physics, Gaußstraße 20, Wuppertal, Germany

[b] Observatorio Pierre Auger, Av. San Martín Norte 304, 5613 Malargüe, Argentina

ONLINE ICRC 2021
THE ASTROPARTICLE PHYSICS CONFERENCE
Berlin | Germany
37th International Cosmic Ray Conference
12–23 July 2021

SPONSORED BY THE Federal Ministry of Education and Research

PIERRE AUGER OBSERVATORY

Key features of UHECR flux above the ankle

- Above the ankle at 5 EeV, flux long thought to be primarily extragalactic in origin. Ex: (Linsley 1963)
- Supported by the Dipole above 8 EeV (Aab et al. 2017) → Ex: see (C. Ding, this conference #1415)
- Further supported by evidence of anisotropies above 32 EeV (J. Biteau, this conference #511)
- Above the ankle, the composition is well described as intermediate in mass and mixed (Bellido 2018) and (E. Guido, this conference #547)

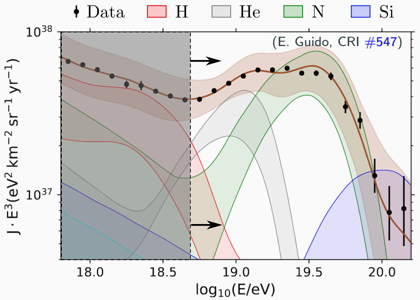

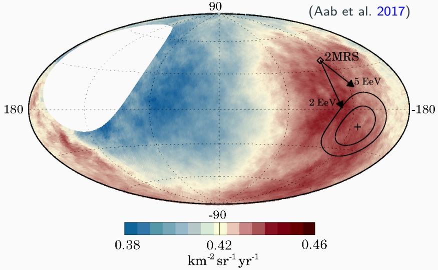

Higher mass primaries from the Galactic plane

- (Erdmann et al. 2016) showed definite transition from diffusive to ballistic propagation in GMF around 6 EV
- (Farrar and Sutherland 2019) showed GMF obscures sources and lenses their images off the plane
- (Farrar 2014) showed effect where images of off-plane sources are lensed toward the plane
- Effect depends on primary rigidity
  - → no effect on diffusely propagating particles
  - → deflection starts around ballistic rigidity threshold
  - → weakens for higher rigidity particles
- UHECR composition mixed, therefore as energy climbs:
  - → effect starts then weakens for light primaries
  - → kicks in for progressively heavier component
  - → heaviest components diffusive ⇝ isotropic

(Farrar and Sutherland 2019)

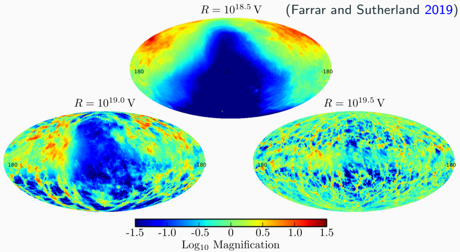

Relative magnification based on source position

(Farrar 2014)

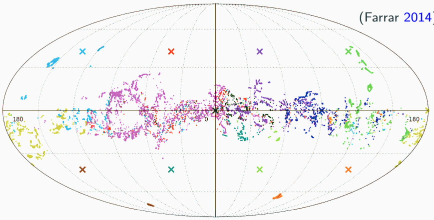

Lensing of off plane sources – proton 10 EeV

Step-by-step testing method

1. Measure the atmospheric depths of shower maximum, $X_{\rm max}$, using the hybrid method outlined in (Aab et al. 2014) and specifically (Yushkov 2020)
2. Remove the $X_{\rm max}$ elongation rate so events over a threshold energy, $E_{\rm min}$, can be combined
3. Define the on- and off-plane regions using some Galactic latitude splitting angle $b_{\rm split}$

   $$\text{On-plane: } |\ b_i\ | \leq b_{\rm split} \qquad \text{Off-plane: } |\ b_i\ | > b_{\rm split}$$

4. Obtain a Test Statistic comparing the on- and off-plane $X_{\rm max}$ distributions using the Anderson-Darling 2-Sample test (Anderson and Darling 1952)
5. Perform a scan over a subset of the data to select $E_{\rm min}$ and $b_{\rm split}$ prescription.
6. Apply the scan selected thresholds as a prescription to remaining data (01.01.2013- 31.12.2018)
7. Calculate statistical significance using Monte-Carlo and random skies
8. Evaluate systematic uncertainties

BERGISCHE UNIVERSITÄT WUPPERTAL

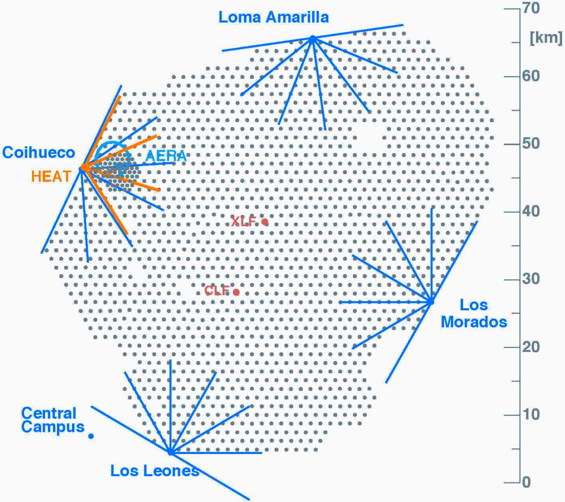

The Pierre Auger Observatory

- FD: 27 fluorescence telescopes
- SD: 1660 water-Cherenkov detectors
- Hybrid measurement concept:
  - → Core timing/location with SD
  - → Geometry with FD pixel trace
  - → Energy and X_{max} from FD light profile

Event X_{max} values obtained using:

the reconstruction, selection, and methods from (Yushkov 2020) on hybrid data collected between 01.12.2004–31.12.2018

- see backup for details -

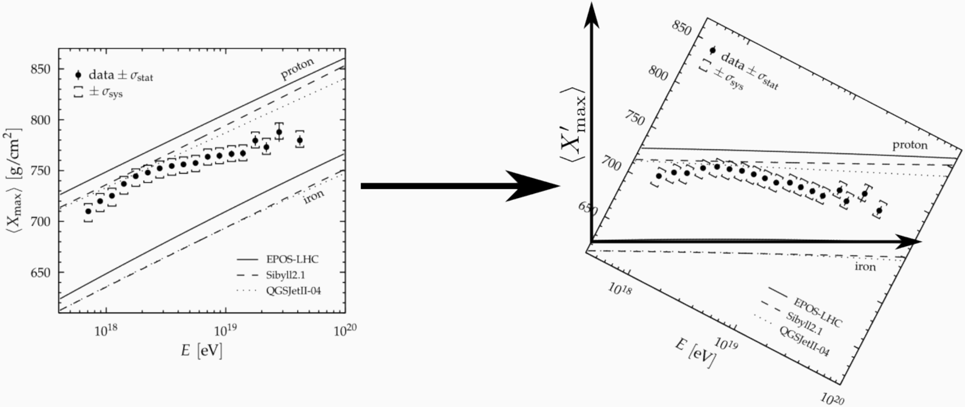

$$X'_{max} = X_{max} - \underbrace{\left(649 + 63.1 \log_{10}\left(E_{rec}/\,\mathrm{EeV}\right) + 1.97 \log_{10}\left(E_{rec}/\,\mathrm{EeV}\right)^2\right)}_{\text{EPOS-LHC elongation rate for iron}}$$

Choice of hadronic model has insignificant influence on end result (≈ 0.02 g/cm²)

BERGISCHE UNIVERSITÄT WUPPERTAL

Data-driven selection of energy and latitude thresholds

- Scan over the data recorded before 01.01.2013 (54 %)
- 5° steps in b and 0.1 lg(E/eV) steps in energy
- Highest TS of 8.35 for: $\rightarrow E_{\text{min}} = 10^{18.7}$ eV
  $\rightarrow b_{\text{split}} = 30°$

Set as prescription for remaining data

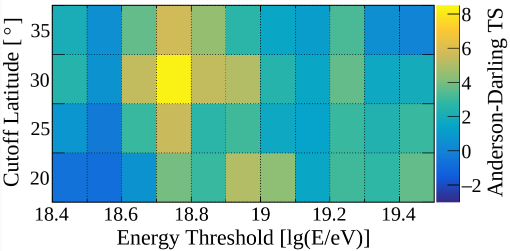

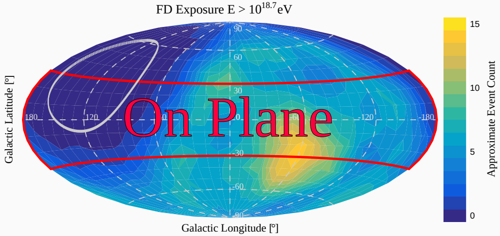

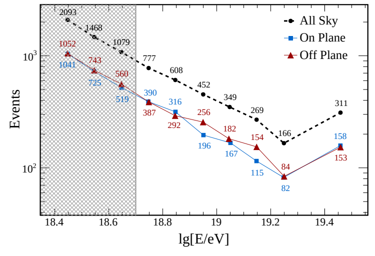

On- and off-plane X_{max} difference in remaining data

BERGISCHE UNIVERSITÄT WUPPERTAL

Unscanned data: $TS = 12.6$

$\Delta\langle X'_{max}\rangle = 10.5 \pm 2.5^{+2.1}_{-2.2}\ \mathrm{g/cm^2}$

$\Delta\sigma(X'_{max}) = 5.9 \pm 3.1^{+3.5}_{-2.5}\ \mathrm{g/cm^2}$

All data: $TS = 21.0$

$\Delta\langle X'_{max}\rangle = 9.1 \pm 1.6^{+2.1}_{-2.2}\ \mathrm{g/cm^2}$

$\Delta\sigma(X'_{max}) = 5.9 \pm 2.1^{+3.5}_{-2.5}\ \mathrm{g/cm^2}$

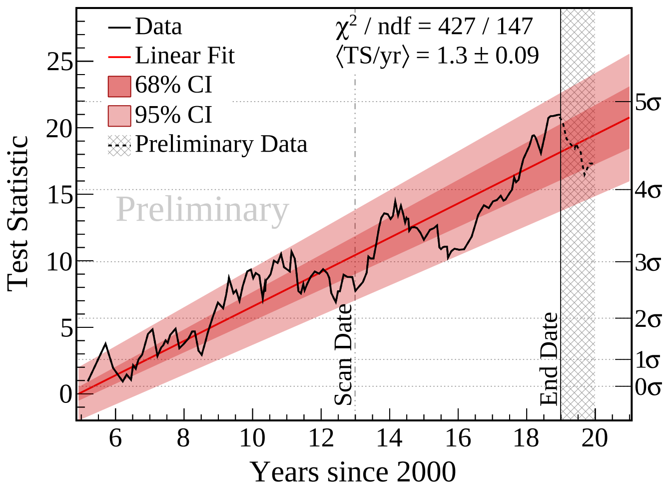

BERGISCHE UNIVERSITÄT WUPPERTAL

Statistical significance is calculated by duplicating the analysis on many random skies

- The data is shuffled in arrival direction to form random skies for each MC trial from which TS are extracted
- Scan duplicated in all data test
  $\rightarrow$ Imposes heavy penalization (only 0.5 σ gained)
- 1E9 MC trails for unscanned data (< 1 % uncertainty)
- 1E10 MC trails for full dataset (< 1 % uncertainty)

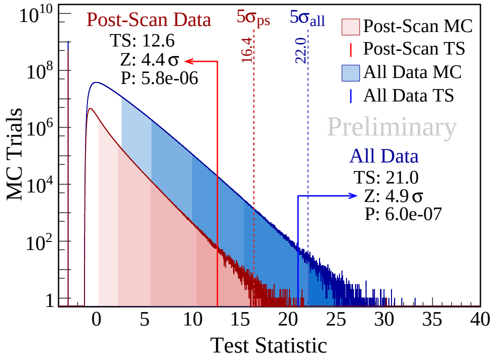

Unscanned data:
Stat. Significance 4.4 σ
Chance probability 1 in 172,000

All available data:
Stat. Significance 4.9 σ
Chance probability 1 in 1,678,000

BERGISCHE UNIVERSITÄT WUPPERTAL

Systematic effects which apply equally to both regions will cancel in a comparison between them

- Local event arrival geometries, camera signatures and atmospheric conditions very similar
- Same detectors, reconstruction method and analysis technique for both regions

Only non-canceling sources of systematic uncertainty:

1. Selection and reconstruction uncertainties
2. Seasonal variation of exposure and aerosols
3. Instrumentation differences between FD sites

Total systematic uncertainty:

$^{+2.10}_{-2.23}$ g/cm^2 for $\Delta\langle X'_{\max}\rangle$ (Off-On)

$^{+3.49}_{-2.48}$ g/cm^2 for $\Delta\sigma(X'_{\max})$ (Off-On)

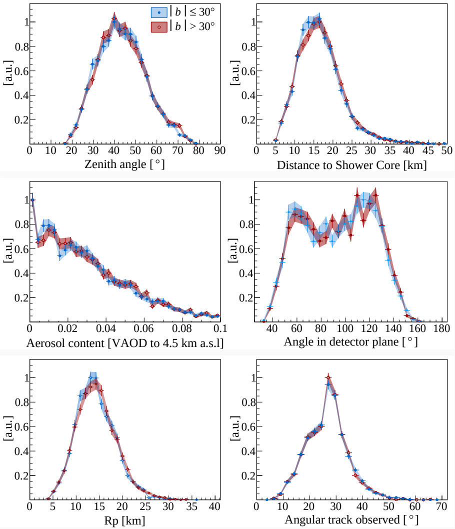

Significance considering systematic uncertainties

- On/Off-plane mean X_{max} difference is $4.1 \times$ the systematic uncertainty
- On/Off-plane RMS difference is $2.4 \times$ the systematic uncertainty
- Impact of the systematic uncertainty on significance estimated by randomly sampling from them to decrease on/off-plane difference on an event-by-event basis
- 1 million trials gives a lower bound TS of 11.2

→ **at least 3.3 σ with systematic effects** taken as the resultant confidence level.

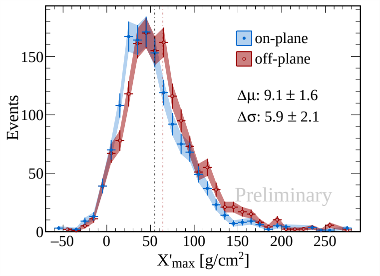

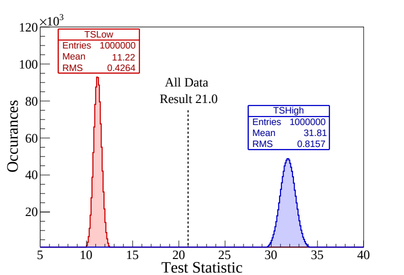

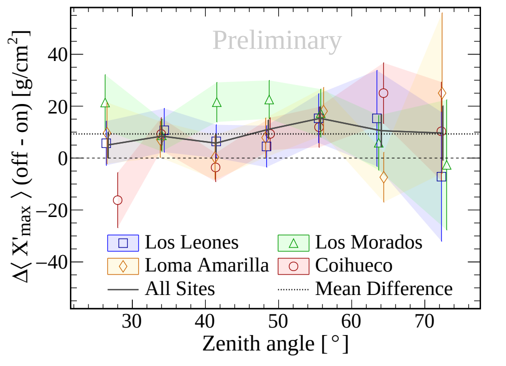

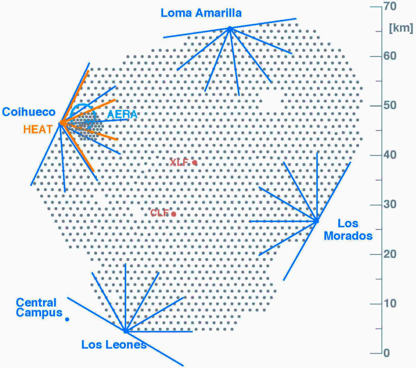

On/Off difference independently seen in all FD sites and 22/28 zenith bins

Because each FD site FoV differs by 90° Systematic causes can not easily explain the on/off difference.

Composition Plots

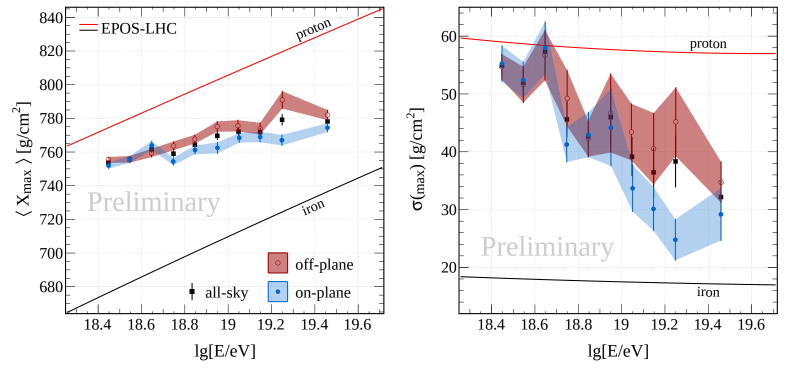

Good separation for above $10^{18.7}$ eV

Indicates a heavier mean mass on-plane for all energies above the ankle

Map compares $\langle X_{\max} \rangle$ of events within 30° of each bin to the rest of the sky

Red: lower mass than rest of sky
Blue: higher mass than rest of sky

- TS is Welch's T-Test applied to in- and out-of-hat $X'_{\max}$ distributions (Welch 1938)
- Detector/analysis effects corrected for by event arrival declination

$E \geq 10^{18.7}$ eV

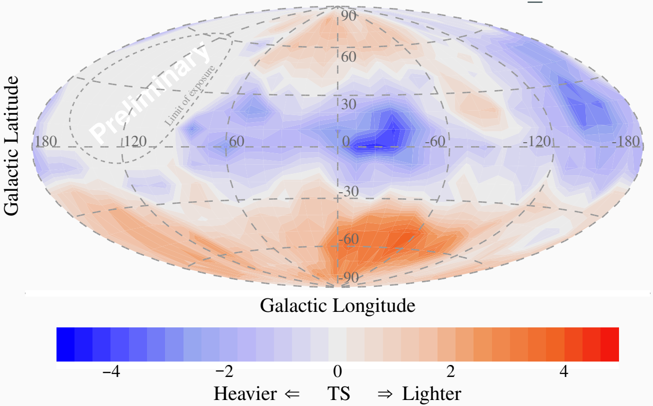

- Verifies a mixed composition above the ankle.
- Suggests GMF could cause composition anisotropies
  → However, a causal relationship with the GMF is not required
- Unrelated anisotropy may have instead been captured by lucky use of the Galactic plane as a catalog
  → Mass-dependent horizons can create composition anisotropies à la (Globus, Allard, and Parizot 2008)
  → In any case, a combination of several effects is likely
- Due to impending changes to our standard X_{max} reconstruction, results are preliminary
  → New general FD X_{max} publication in preparation
  → Publication in preparation

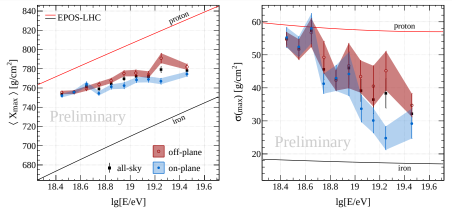

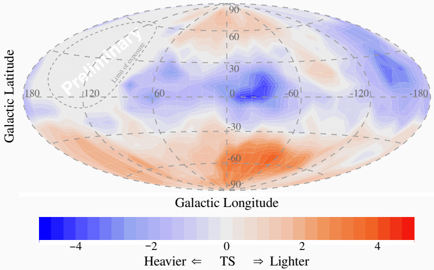

Thanks for you interest!

Don't miss the discussion session on July 13th at 18:00 CEST

See backup slides for:

- References
- Further motivation
- X_{max} reconstruction details
- Systematic checks
- RA/Dec Sky Map

References

Aab, Alexander et al. (2014). "Depth of Maximum of Air-Shower Profiles at the Pierre Auger Observatory: Measurements at Energies above $10^{17.8}$ eV". In: PRD 90.12, p. 122005. DOI: 10.1103/PhysRevD.90.122005.

– (2017). "Observation of a Large-scale Anisotropy in the Arrival Directions of Cosmic Rays above 8×10^{18} eV". In: Science 357.6537, pp. 1266–1270. DOI: 10.1126/science.aan4338.

Bellido, Jose (2018). "Depth of maximum of air-shower profiles at the Pierre Auger Observatory". In: PoS ICRC2017. Ed. by Darko Veberic, p. 506. DOI: 10.22323/1.301.0506.

Erdmann, Martin et al. (2016). "The Nuclear Window to the Extragalactic Universe". In: Astropart. Phys. 85, pp. 54–64. DOI: 10.1016/j.astropartphys.2016.10.002.

Farrar (2014). "The Galactic magnetic field and ultrahigh-energy cosmic ray deflections". In: C R Phys 15.4, pp. 339–348.

Farrar and Sutherland (2019). "Deflections of UHECRs in the Galactic magnetic field". In: JCAP 05, p. 004. DOI: 10.1088/1475-7516/2019/05/004.

Globus, N., D. Allard, and E. Parizot (2008). "Propagation of high-energy cosmic rays in extragalactic turbulent magnetic fields: resulting energy spectrum and composition". In: Astron. Astrophys. 479, p. 97. DOI: 10.1051/0004-6361:20078653.

Jansson, Ronnie and Glennys R. Farrar (2012). "A New Model of the Galactic Magnetic Field". In: ApJ. 757, p. 14. DOI: 10.1088/0004-637X/757/1/14.

Linsley, John (1963). "Primary cosmic rays of energy 10**17 to 10**20-eV: The energy spectrum and arrival directions". In: ICRC 8 77.

Pshirkov, M. et al. (2011). "Deriving global structure of the Galactic Magnetic Field from Faraday Rotation Measures of extragalactic sources". In: Astrophys. J. 738, p. 192. DOI: 10.1088/0004-637X/738/2/192.

Welch, Bernard L (1938). "The significance of the difference between two means when the population variances are unequal". In: Biometrika 29.3/4, pp. 350–362. DOI: 10.2307/2332010.

Mass Composition of Cosmic Rays with Energies above $10^{17.2}$ eV from the Hybrid Data of the Pierre Auger Observatory (2020).
Vol. ICRC2019, p. 482. DOI: 10.22323/1.358.0482.

Composition Sky Map - RA/Dec

BERGISCHE UNIVERSITÄT WUPPERTAL

$E \geq 10^{18.7}$ eV

Map compares $\langle X_{\text{max}} \rangle$ of events within 30° of each bin to the rest of the sky

Red: lower mass than rest of sky
Blue: higher mass than rest of sky

- TS is Welch's T-Test applied to in- and out-of-hat X'_{max} distribution
- Detector/analysis effects corrected for by event arrival declination

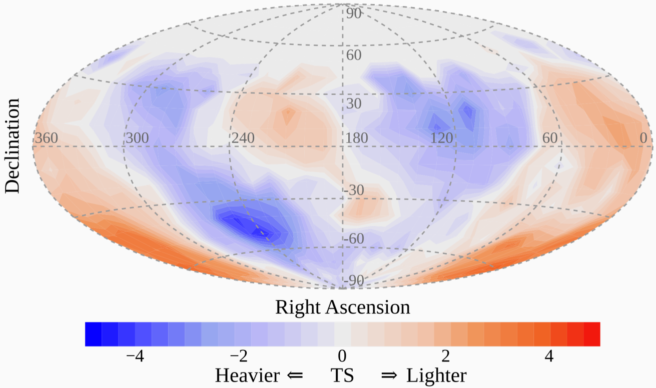

Motivating mass dependent anisotropies

- (Erdmann et al. 2016) showed transition from diffusive to ballistic propagation in the GMF around 4 - 6 EV using both JF12 (Jansson and G. R. Farrar 2012) and PTK11 (Pshirkov et al. 2011)
- Threshold dependence on Galactic latitude of CR
- At fixed energy above this limit:
  High mass → diffusive → isotropic arrival
  Low mass → ballistic → preserve some source anisotropy
- Differing horizon of each primary species introduces potential of differing source distributions (Globus, Allard, and Parizot 2008)

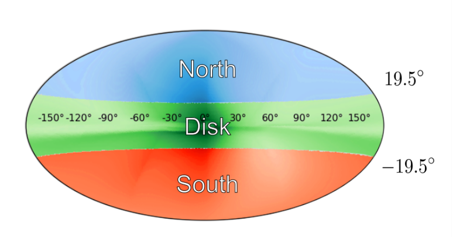

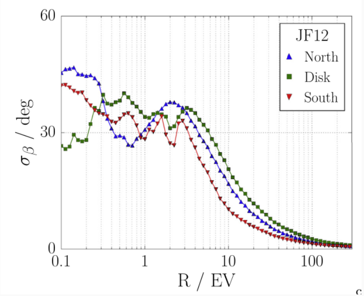

(Erdmann et al. 2016)

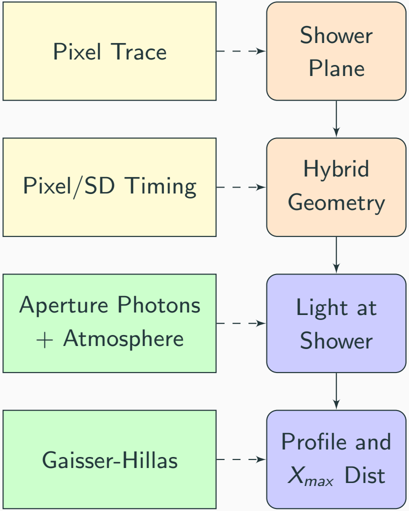
Pixel Trace
Shower Plane
Pixel/SD Timing
Hybrid Geometry
Aperture Photons + Atmosphere
Light at Shower
Gaisser-Hillas
Profile and X_{max} Dist

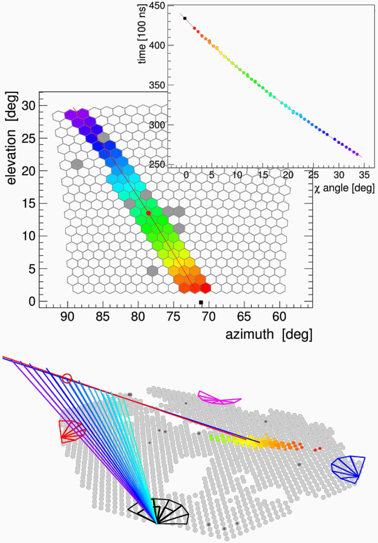
time [100 ns]
450
400
350
300
250
0 5 10 15 20 25 30 35
χ angle [deg]
elevation [deg]
30
25
20
15
10
5
0
90 85 80 75 70 65 60
azimuth [deg]

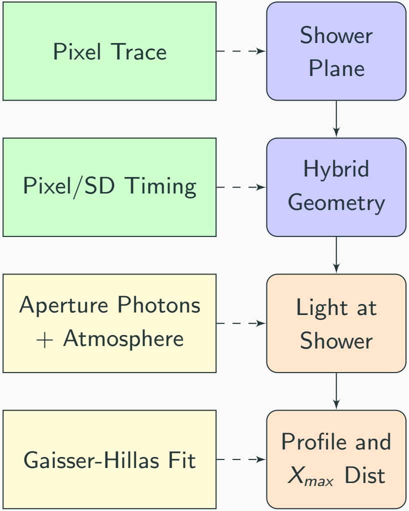

Pixel Trace
Shower Plane
Pixel/SD Timing
Hybrid Geometry
Aperture Photons + Atmosphere
Light at Shower
Gaisser-Hillas Fit
Profile and X_{max} Dist

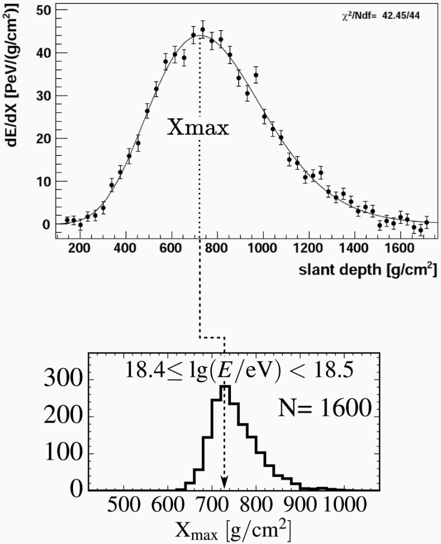

dE/dX [PeV/(g/cm²)]
χ²/Ndf= 42.45/44
Xmax
slant depth [g/cm²]
0 10 20 30 40 50
200 400 600 800 1000 1200 1400 1600
18.4≤ lg(E/eV) < 18.5
N= 1600
0 100 200 300
500 600 700 800 900 1000
Xmax [g/cm²]

BERGISCHE UNIVERSITÄT WUPPERTAL

Quality Selection Criteria:

- Full instrumentation functionality, no clouds and clear atmosphere
- Long tracks in detector (20°) with X_{max} in FoV with a low fit χ^2

Fiducial Selection Criteria:

- Surface Detector proton trigger probability > 0.9
- Surface Detector proton - iron trigger efficiency difference < 0.05
- FD Fiducial FoV cuts to flatten X_{max} acceptance

Post-cut X_{max} distribution still differs from true X_{max} distribution due to resolution, and detector acceptance.

$$f_{obs}(X_{max}^{rec}) = \int_0^{\infty} f_{true}(X_{max})\varepsilon(X_{max})R(X_{max}^{rec} - X_{max})dX_{max}$$

Field of View and X_{max} Acceptance

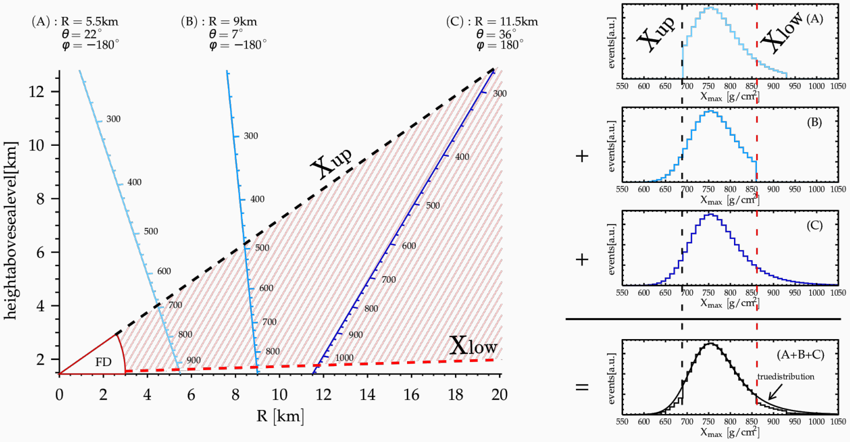

(Aab et al. 2014)

X_{max} must be in FoV to pass quality cuts

Geometry determines which X_{max} values will be measured.

Fiducial FoV Cuts

Distributions biased when
$X_{low}^{fid} < X_{low}$ or FoV top $X_{up}^{fid} > X_{up}$

(Aab et al. 2014)

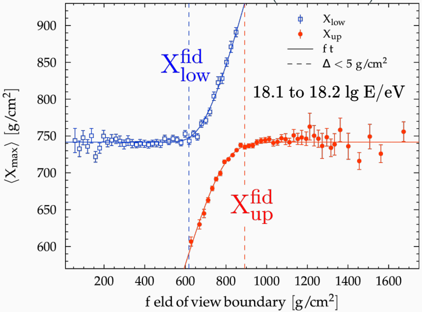

(Aab et al. 2014)

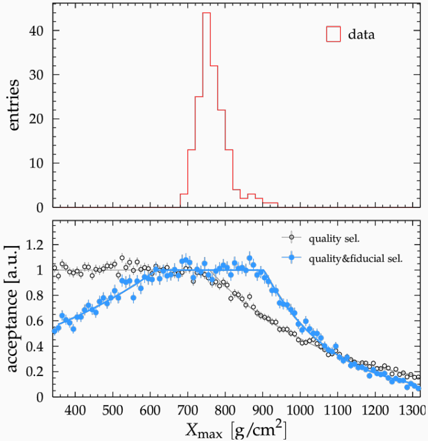

Fiducial cut flattens X_{max} acceptance for the majority of selected events.
Events with non-flat acceptance up-weighted via acceptance parameterization

X_{max} acceptance of on- and off-plane probed with Sibyll-2.3c CONEX showers (p, Fe) with the profile shifted so that $X_{max} \in [300, 1500]\,\text{g/cm}^2$ is sampled evenly

- Detector simulations account for time dependent state of the detector
- On- and off-regions corrected separately
  $\rightarrow$ weighting method from 2014 PRD employed (Aab et al. 2014)
- 1.4 % events in data have less than full acceptance

Detector and selection acceptance agree well within uncertainties

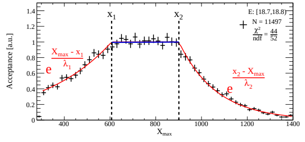

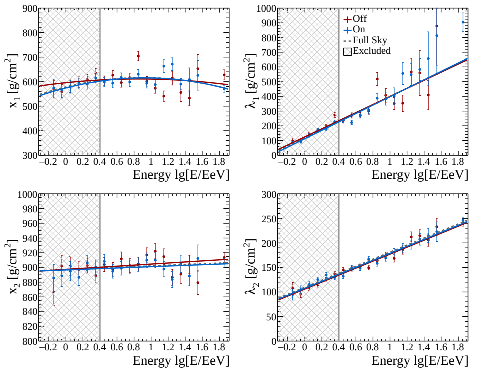

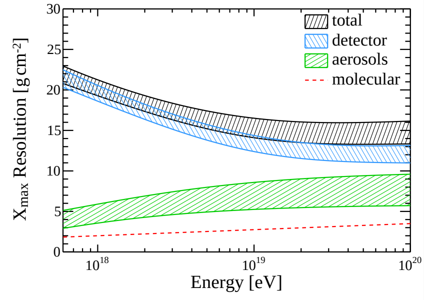

X_{max} Resolution

Effects from the atmosphere and the detector are combined into the X_{max} resolution to correct the X_{max} distributions.

Systematic uncertainties from the atmosphere, FD calibration reconstruction and detector are summed for systematic error of the moments

(Aab et al. 2014)

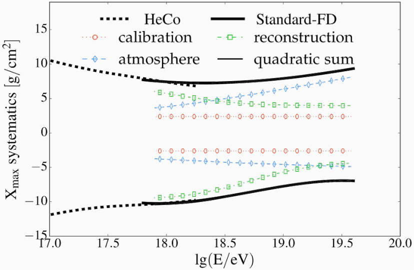

Systematic uncertainty of X_{max} scale

X_{max} Reconstruction bias and resolution On/Off-plane

X_{max} rec. bias and resolution on- and off-plane probed with 4-component (H, He, N, Fe) Sibyll-2.3c CONEX showers

- Detector simulations account for time dependent state of the detector
- Components reweighed to (Bellido 2018) mass fractions by energy
- Event-by-event comparison of reconstructed X_{max} to MC truth
- On- and off-regions each corrected by their energy parameterization

Reconstruction bias and resolution agree well within uncertainties

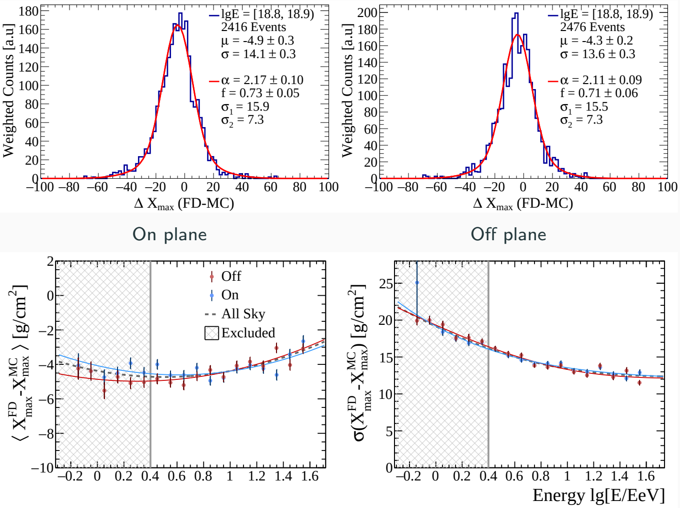

Systematic Error Summary from (Aab et al. 2014)

Error Source	Ref.	$\langle X_{max} \rangle$ Error [g/cm^2] 18.4 lg(E/eV)	19.6 lg(E/eV)	Applies to comparative analysis?
Detector Calibration		$\sim \pm 3$		
SD-FD Timing Offset		$\leq \pm 2$		no: applies to all events
Pixel Calibration		$\leq \pm 1$		**yes: Eye-to-Eye differences**
Telescope Alignment		$\leq \pm 1$		**yes: Eye-to-Eye differences**
Reconstruction		$^{+4.3}_{-8.2}$	$^{+4.0}_{-4.2}$	
Reconstruction Bias		0		**yes: sky region differences**
Profile Fit Function		± 4		no: applies to all events
Lateral Width Correction		$^{+1.6}_{-7.1}$	$^{+0.1}_{-1.3}$	no: On/Off Plane geometric similarity
Atmosphere		$\leq ^{+4.6}_{-3.8}$	$\leq ^{+7.5}_{-4.7}$	
Fluorescence yield		± 0.4		no: applies to all events
Multiple Scattering		$\leq \pm 2$		no: On/Off Plane geometric similarity
VAOD Systematics		± 1.6	± 2	**yes: seasonal variation of VAOD**
VAOD Uniformity		± 2.8	± 3.7	
VAOD Normalization		$+2.5$	$+6.5$	
Other		$\leq ^{+2.5}_{-1.5}$		
X_{max} **Acceptance**		$\leq \pm 1.5$		**yes: sky region differences**
Invisible energy		$\leq +1.2$		no: applies to all events
Total from dedicated studies		$\leq ^{+2.60}_{-2.18}$	$\leq ^{+3.80}_{-2.77}$	**see below**

Source	Uncertainty [g/cm^2] $\Delta\langle X_{max}\rangle$	Uncertainty [g/cm^2] $\Delta\sigma(X_{max})$
X_{max} Acceptance	$^{+1.14}_{-0.71}$	$^{+2.37}_{-1.61}$
Rec. Bias	± 0.36	± 0.01
Rec. Resolution	**0**	$^{+1.78}_{-0.24}$
Seasonal variation	$^{+1.00}_{-1.53}$	$^{+1.19}_{-1.23}$
Instrumentation	± 1.41	± 1.41
Sum in Quadrature	$^{+2.10}_{-2.23}$	$^{+3.49}_{-2.48}$

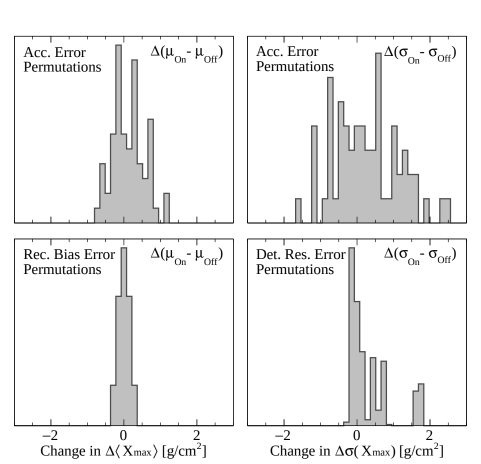

Changes to the magnitude of the end result using a permutation of all parameterization errors

Source	Uncertainty [g/cm^2] $\Delta\langle X_{\mathrm{max}}\rangle$	$\Delta\sigma(X_{\mathrm{max}})$
X_{max} Acceptance	$^{+1.14}_{-0.71}$	$^{+2.37}_{-1.61}$
Rec. Bias	± 0.36	± 0.01
Rec. Resolution	0	$^{+1.78}_{-0.24}$
Seasonal variation	$^{+1.00}_{-1.53}$	$^{+1.19}_{-1.23}$
Instrumentation	± 1.41	± 1.41
Sum in Quadrature	$^{+2.10}_{-2.23}$	$^{+3.49}_{-2.48}$

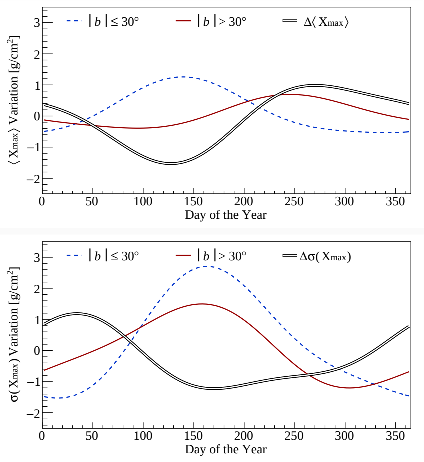

Observed variation of the first two moments of the on- and off-plane X_{max} distributions weighted by exposure.

Source	Uncertainty [g/cm^2] $\Delta\langle X_{max}\rangle$	$\Delta\sigma(X_{max})$
X_{max} Acceptance	$^{+1.14}_{-0.71}$	$^{+2.37}_{-1.61}$
Rec. Bias	± 0.36	± 0.01
Rec. Resolution	0	$^{+1.78}_{-0.24}$
Seasonal variation	$^{+1.00}_{-1.53}$	$^{+1.19}_{-1.23}$
Instrumentation	± 1.41	± 1.41
Sum in Quadrature	$^{+2.10}_{-2.23}$	$^{+3.49}_{-2.48}$

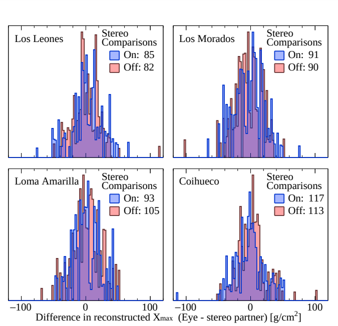

Site	events	Off − On plane bias $\langle X_{max}\rangle$	$\sigma(X_{max})$
LL	167	-0.8 ± 3.7	-3.2 ± 2.5
LM	181	-1.1 ± 3.7	-1.0 ± 2.5
LA	198	-0.1 ± 3.2	$+0.7 \pm 2.2$
CO	230	**3.0 ± 3.1**	-2.5 ± 2.1

Comparisons of on- and off-plane X_{max} reconstructions between FD-sites using stereo events.

Backup X_{max} Drift and On/Off Signal

Energy normalized FidFoV X_{max} on- and off-plane plotted separately vs time.

- Points are sets of 10 events
- Lines are cumulative means
- Solid fill is the running average over surrounding 40 events

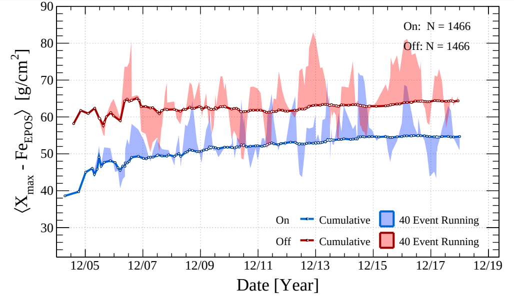

Both On and Off separately display a similar trend to those seen in other studies

No apparent affect on result.

BERGISCHE UNIVERSITÄT WUPPERTAL

$$z_i = X_{max}^{norm} = X_{\max i} - EPOS_{Fe}(E_i)$$

Anderson-Darling 2 Sample Homogeneity Test

$$TS_{\mathrm{AD}} = \frac{n-1}{n^2} \sum_{i=1}^{2} \left[\frac{1}{n_i} \sum_{j=1}^{L} h_j \frac{\left(nF_{ij} - n_i H_j\right)^2}{H_j\left(n - H_j\right) - \frac{1}{4} n h_j} \right]$$

Modification to add sensitivity to distribution ordering

$$TS = \begin{cases} TS_{\mathrm{AD}} & : \langle X_{max}^{norm} \rangle^{on} < \langle X_{max}^{norm} \rangle^{off} \\ -3 & : else \end{cases},$$

n size of pooled sample

n_i size of sample i

z_j the value of the j^{th} event in the combined data set ordered from smallest value to largest

h_j is number of events in the pooled sample with a value equal to z_j

H_j is number of events in the pooled sample with a value less than $z_j + \frac{1}{2} h_j$

F_{ij} is number of events in the i^{th} sample with a value less than $z_j + \frac{1}{2} h_j$